Supporting Information: Trade-Offs between Speed, Accuracy, and Dissipation in tRNA$^{\mathbf{Ile}}$ Aminoacylation

Qiwei Yu,[1,2] Joel D. Mallory,[2] Anatoly B. Kolomeisky,[2,3,4,5] Jiqiang Ling,[6] and Oleg A. Igoshin[2,3,7,8,*]

[1] *School of Physics, Peking University, Beijing 100871, China*

[2] *Center for Theoretical Biological Physics, Rice University, Houston, TX 77005*

[3] *Department of Chemistry, Rice University, Houston, TX 77005*

[4] *Department of Chemical and Biomolecular Engineering, Rice University, Houston, TX 77005*

[5] *Department of Physics and Astronomy, Rice University, Houston, TX 77005*

[6] *Department of Cell Biology and Molecular Genetics, The University of Maryland, College Park, MD 20742, USA*

[7] *Department of Bioengineering, Rice University, Houston, TX 77005*

[8] *Department of Biosciences, Rice University, Houston, TX 77005*

I. CHEMICAL NETWORK FOR THE tRNA$^{\mathbf{Ile}}$ AMINOACYLATION

In this section, we provide a more detailed account on our model of the mechanism of aminoacylation by IleRS , including the derivation of the biochemical parameters in the model. The aminoacylation mechanism can be divided into two stages [1, 2]. In the first stage, the amino acid (aa) is activated at the active site of the synthetase by hydrolyzing ATP to form aminoacyl-adenylates (Ile-AMP or Val-AMP), as shown by the reactions in the green box (see Figure S1). The tRNA can subsequently bind to the complex. The charged amino acid is then transferred to the 3' end of the tRNA, which is represented by the reactions in the purple box (see Figure S1). Finally, the charged aminoacyl-tRNA dissociates from the synthetase at rate k_p (or k_p') and is delivered to the ribosome by the elongation factor Tu (EF-Tu). Since we are mainly concerned with the accuracy of tRNA charging, the delivery and any subsequent process will not be included in the model.

The amino acid substrate specificity is achieved not only by the preferential binding of the

* igoshin@rice.edu

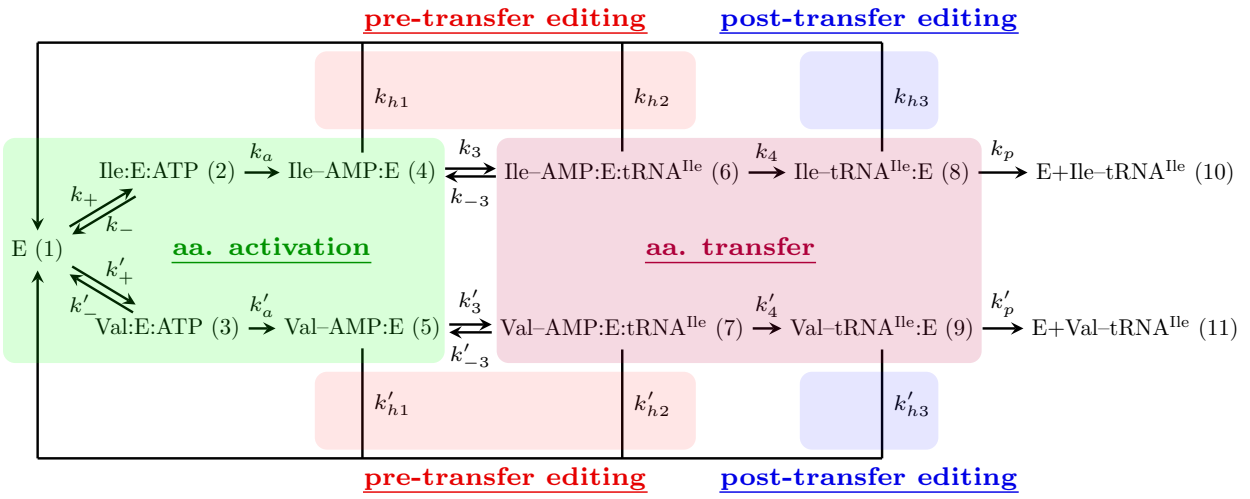

FIG. S1. Chemical reaction network for the aminoacylation of tRNA^{Ile} in *E. coli*. Abbreviations: E, isoleucyl-tRNA synthetase (IleRS); Ile, isoleucine; Val, valine. The rate constants are labeled k_i for the right pathway (isoleucine pathway) and k'_i for the wrong pathway (valine pathway). The three proofreading pathways are labeled as k_{h1}, k_{h2}, k_{h3}, and their primed counterparts. The chemical states are numbered from 1 to 11 as indicated by the numbers in the parentheses.

cognate amino acid, but also through selective editing mechanisms [2, 3]. Although these proofreading pathways mainly serve to reduce the production rate of misacylated tRNA, they can also occur (albeit with lower probability) for complexes with the right amino acid. Therefore, we construct a completely symmetric reaction network where all proofreading mechanisms exist for both amino acids. The preference for the cognate substrate is reflected in the higher affinity and lower editing rates. Specifically, there are two pre-transfer editing pathways (red boxes in Figure S1) and one post-transfer editing pathway (blue boxes in Figure S1). The first pre-transfer editing (modeled by k_{h1}) is tRNA-independent and occurs before tRNA binding. In this reaction, the aminoacyl-adenylate (aa-AMP) is either dissociated from the synthetase or hydrolyzed at the active site . We do not distinguish dissociation from hydrolysis because the synthetase is reset to its initial state (E) after either reaction. The second pre-transfer editing pathway (modeled by k_{h2}) is tRNA-dependent and hydrolyzes the aa-AMP complex before the amino acid could be transferred to tRNA, which is already bound to the complex. Finally, the post-transfer editing pathway (modeled by k_{h3}) occurs after the transfer and results in the translocation of aminoacyl-tRNA from the active site to the editing site and its subsequent hydrolysis (deacytlation). We are

only concerned with the proofreading of aminoacyl-tRNA that occurs prior to its release from the aminoacyl-tRNA synthetase. Quality control mechanisms that take place after the aminoacyl-tRNA is released (e.g., the preferential binding of the elongation factor Tu to the correctly acylated-tRNA[2]) constitute a different layer of specificity enhancement and hence, are not explicitly considered in the model. The model focuses on the stochastic dynamics of a single isoleucyl-tRNA synthetase and assumes constant concentrations of other molecular species in the cellular environment such as amino acids. Although the low activation energy for the hydrolysis of the ester bond of aa-tRNA allows for the deacylation of misacylated products by either editing site residues or the free-hydroxyl groups of A76 [2], they are not relevant in this current framework.

The above-described mechanism is illustrated on Figure S1 and serves as foundation for our biophysical model. The rate parameters are either directly obtained or indirectly derived from published kinetic experiments [3–18] as described below.

A. Determination of Rate Constants from the Literature

The numeric values and sources of all rate constants that are shown in Figure S1 are summarized in Table S1. Most of them are directly obtained from the literature. Explanations for a few of parameters that are indirectly derived or estimated are listed below:

- The tRNA binding steps (k_3 and k_3') are assumed to be diffusion-limited. Their forward rates are estimated by the Smoluchowski equation $k = 4\pi DR$, where D and R are the diffusion coefficient and the radius of the molecule. There backward rate constants are calculated as the product of the dissociation constant and the forward rate constant.

- The binding of amino acid and ATP are model as one step with the assumption that ATP binding is diffusion-limited. The detailed procedures are given in the next subsection.

- Product release rate is derived by using the the three slowest steps to estimate the waiting time $\tau = \frac{1}{k_{obs}} \approx \frac{1}{k_4} + \frac{1}{k_p} + \frac{1}{k_a}$, from which k_p can be solved. k_{obs} is given by Table 4 of ref. [13].

- The product release rate for the non-cognate substrate k_p' is assumed to be the same as the cognate product release rate k_p based on a chemical argument. Given that

valine and isoleucine differ only in the side chain (which is a small part of the whole aminoacyl-tRNA complex) and that the amino acid has been transferred to the tRNA, we argue that this difference should not affect the product release rate.

Parameter	Value (s^{-1})	Sources
k_+	6.2×10^5	[3, 5, 14, 15]
k_-	30	[3, 5, 14, 15]
k'_+	7.0×10^3	[3, 5, 14, 15]
k'_-	28	[3, 5, 14, 15]
k_a	40	k_{cat} from [3]
k'_a	31	k_{cat} from [3]
k_3	8.7×10^2	[8, 17, 18]
k_{-3}	1.1×10^2	[4, 17, 18]
k'_3	8.7×10^2	[8, 17, 18]
k'_{-3}	1.1×10^2	[4, 17, 18]
k_4	3.8	Figure 2 of [3]
k'_4	2.3	Figure 2 of [3]
k_{h_1}	0.003	Table 1 of [3]; Supp. Table 1 of [13]
k'_{h_1}	0.036	Table 1 of [3]; Supp. Table 1 of [13]
k_{h_2}	0.0135	Table 1 of [3]
k'_{h_2}	0.128	Table 1 of [3]
k_{h_3}	0.058	Table 4 of [3]
k'_{h_3}	64	Table 4 of [3]
k_p	0.65	Table 4 of [13]
k'_p	0.65	Table 4 of [13]

TABLE S1. Estimated first-order kinetic parameters involved in the $tRNA^{Ile}$ aminoacylation model.

B. Justification for Modeling Amino Acid Binding and ATP Binding as One Step

The first step of our kinetic model (Figure 1) is the charging of the amino acid. It includes binding of both the amino acid and ATP to the enzyme followed by transfer of AMP to the amino acid and release of the pyrophosphate PP_i. Generally speaking, the amino acid and ATP don't have to bind sequentially. Here, we construct a one-step binding model with effective first-order reaction rates k_+ and k_- under physiological conditions by exploring the complete model in which ATP or the amino acid bind in random order.

First, we consider a sequential binding model (s_1 is the amino acid and s_2 is ATP),

$$\mathrm{E} \underset{k_{-1}}{\overset{k_1 s_1}{\rightleftharpoons}} \mathrm{E}{\cdot}s_1 \underset{k_{-2}}{\overset{k_2 s_2}{\rightleftharpoons}} \mathrm{E}{\cdot}s_1 \cdot s_2 \cdot$$

Using x, y, and z to denote the concentration of the three states of the enzyme, the quasi-steady-state approximation of $\mathrm{E}{\cdot}s_1$ reads:

$$(k_2 s_2 + k_{-1})y = k_1 s_1 x + k_{-2} z. \tag{S1}$$

The net flux through this pathway is

$$J = k_1 s_1 x - k_{-1} y = k_1 s_1 x - k_{-1} \frac{k_1 s_1 x + k_{-2} z}{k_2 s_2 + k_{-1}} = \frac{k_1 s_1 k_2 s_2 x - k_{-2} k_{-1} z}{k_2 s_2 + k_{-1}}, \tag{S2}$$

so we can view this model as a single step reaction with:

$$\mathrm{E} \underset{J_- = \frac{k_{-2}k_{-1}}{k_2 s_2 + k_{-1}}}{\overset{J_+ = \frac{k_1 k_2 s_1 s_2}{k_2 s_2 + k_{-1}}}{\rightleftharpoons}} \mathrm{E}{\cdot}s_1 \cdot s_2$$

Note that the forward reaction rate is proportional to $s_1 s_2$, so we can effectively write it as the simultaneous binding of s_1 and s_2. Since the s_1 and s_2 are completely symmetric in this case, we can write the other pathway in which s_2 binds first in the same form and sum the reaction constants together. In the end, we have

$$\mathrm{E} \underset{k_-}{\overset{k_+ s_1 s_2}{\rightleftharpoons}} \mathrm{E}{\cdot}s_1 \cdot s_2 \xrightarrow{k_a} \mathrm{E}{\cdot}\mathrm{aa}{-}\mathrm{AMP},$$

in which $k_+ = \frac{k_1 k_2}{k_2 s_2 + k_{-1}} + \frac{k_3 k_4}{k_4 s_1 + k_{-3}}$ and $k_- = \frac{k_{-1} k_{-2}}{k_2 s_2 + k_{-1}} + \frac{k_{-3} k_{-4}}{k_4 s_1 + k_{-3}}$ are both dependent on the ATP and amino acid concentrations. Mathematically, the total flux can be written in the Michaelis-Menten form

$$v = \frac{k_a e_0}{1 + \frac{k_a + k_-}{k_+ s_1 s_2}}. \tag{S3}$$

To get parameter estimations for this steps from experiments, we refer to Table 6 of ref. [3] where the production of the aa·E·AMP complex is measured by pyrophosphate exchange experiments. The authors fitted to a Michaelis-Menten scheme to their kinetics data with a standard method of determining the Michaelis-Menten constant through a double reciprocal plot ($k_a e_0 v^{-1}$ and $\frac{1}{s_1}$ are plotted against each other). For our scheme, we have

$$\frac{k_a e_0}{v} = 1 + \frac{k_a + k_-}{k_+ s_1 s_2} = 1 + \frac{k_a + k_-}{k_+ s_1 s_2}. \tag{S4}$$

Note that k_+ and k_- are both functions of s_1 and s_2, so the double reciprocal plot is not exactly a straight line. Since the concentration s_1 was varied around K_m in the experiment, the measured Michaelis-Menten constant should be the slope of the tangent near $s_1 = K_m$, mathematically written as:

$$K_m = \frac{d}{ds_1^{-1}} \left(1 + \frac{k_a + k_-}{k_+ s_1 s_2} \right) \Bigg|_{s_1 = K_m}. \tag{S5}$$

Effectively, we are doing a Taylor expansion of Equation S4 near $s_1 = K_m$, whose solution is

$$K_m = \frac{k_a(k_2 s_2 + k_{-1}) + k_{-1}k_{-2}}{k_1 k_2 s_2} = \frac{K_{d1}K_{d2}}{s_2} + \frac{k_a}{k_2 s_2} \left(K_{d1} + \frac{k_2 s_2}{k_1} \right). \tag{S6}$$

Assuming that ATP (s_2) binding is diffusion limiting, the binding rate is

$$k_2 = 4\pi D_{[\mathrm{ATP}]} R_{[\mathrm{ATP}]} = 1.59 \times 10^8\ \mathrm{M^{-1}s^{-1}}, \tag{S7}$$

where D_{ATP} is obtained from [14]; R_{ATP} is obtained from ref. [15]. Considering the physiological concentration of ATP, we have $k_2 s_2 = 1.53 \times 10^6 \mathrm{s^{-1}}$ and $k_{-2} = K_{d,\mathrm{ATP}} k_2 = 2.78 \times 10^4 \mathrm{s^{-1}}$. On the other hand, the experiment measurements are $k_{\mathrm{cat}} = 40.2\ \mathrm{s^{-1}}$ and $K_{\mathrm{M}} = 6.9\ \mu\mathrm{M}$ for isoleucine, and $k'_{\mathrm{cat}} = 31\ \mathrm{s^{-1}}$ and $K'_{\mathrm{M}} = 1.0\ \mathrm{mM}$ for valine. The concentration of ATP used was 4.0 mM. k_1 can be explicitly solved from Equation S6:

$$k_1 = 5.95 \times 10^6\ \mathrm{M^{-1}s^{-1}}(\text{isoleucine}) / 3.2 \times 10^4\ \mathrm{M^{-1}s^{-1}}(\text{valine}). \tag{S8}$$

Hence, $k_1 s_1 = 1.8 \times 10^4\ \mathrm{s^{-1}}(\text{isoleucine}) / 1.3 \times 10^2\ \mathrm{s^{-1}}(\text{valine})$. The reverse rate constant $k_{-1} = k_1 K_{d1} = 48\ \mathrm{s^{-1}}(\text{isoleucine}) / 28\ \mathrm{s^{-1}}(\text{valine})$.

Assuming symmetric rate constants, namely, $k_{\pm 1} = k_{\pm 4}$ and $k_{\pm 2} = k_{\pm 3}$, we then calculate the value of k_+ and k_- under physiological concentrations and use this single step to represent the binding and unbinding of both substrates. The pseudo-first order rate constants are:

$$k_+ = 6.2 \times 10^5\ \mathrm{s^{-1}}(\text{isoleucine}) / 7.0 \times 10^3\ \mathrm{s^{-1}}(\text{valine}) \tag{S9}$$

$$k_- = 30\ \mathrm{s^{-1}}(\text{isoleucine}) / 28\ \mathrm{s^{-1}}(\text{valine}). \tag{S10}$$

C. Thermodynamic Constraints and the Determination of Reverse Reaction Rates

Although some of the steps are strongly driven forward, we make all reactions reversible in the simulation for the sake of thermodynamic consistency as irreversible reactions always lead to infinite dissipation. The rate constants for reverse reactions are determined by a set of thermodynamic constraints that connect the ratio of the rate constants with the chemical potential difference of the reactants and products of any reaction cycle [19]:

$$\Delta\mu = \ln\left(\prod_i \frac{k_{i+}}{k_{i-}}\right), \tag{S11}$$

where k_{i+} and k_{i-} stands for the forward and backward rate constants; $\Delta\mu$ stands for the chemical potential difference between the reactants and products. For futile cycles $\Delta\mu_{\mathrm{ATP}} = 29.5\, k_BT$, and for product formation cycles $\Delta\mu_p = 9.8\, k_BT$. In this system, the thermodynamic constraints read

$$\begin{aligned}
\frac{k_+k_ak_{h1}}{k_-k_{-a}k_{-h1}} &= e^{29.5} \\
\frac{k_+k_ak_3k_{h2}}{k_-k_{-a}k_{-3}k_{-h2}} &= e^{29.5} \\
\frac{k_+k_ak_3k_4k_{h3}}{k_-k_{-a}k_{-3}k_{-4}k_{-h3}} &= e^{29.5} \\
\frac{k_+k_ak_3k_4k_p}{k_-k_{-a}k_{-3}k_{-4}k_{-p}} &= e^{9.8}.
\end{aligned} \tag{S12}$$

The same set of constraints also exist for the noncognate reactions, where the rate constants are simply replaced by their primed counterparts. The reverse rate constants that are omitted in Figure S1 can be determined from these relations. Their values are introduced purely for the calculation of the dissipation and will not change the kinetic behavior of the model.

II. COMPUTATIONAL AND ANALYTIC METHODS

A. Backward Master Equations and the Definitions of Speed and Accuracy

We quantify the speed and accuracy of the aminoacylation process using the framework of a first-passage process [20, 21]. Specifically, the temporal evolution of the system can be considered as Markovian jumps between discrete enzymatic states until the formation of a

correct or incorrect product. In the tRNA^{Ile} aminoacylation network, we have 11 chemical states, which are labeled from 1 to 11 (see Figure S1). States 10 and 11 are end states which correspond to the formation of a correct and incorrect product, respectively. For each state i, we can define $F_{R/W,i}(t)$ as the first-passage probability density such that $F_{R,i}(t)\,\mathrm{d}t$ (or $F_{W,i}(t)\,\mathrm{d}t$) quantifies the probability of forming a correct (or incorrect) product between t and $t+\mathrm{d}t$ without forming any products before time t, assuming that the enzyme starts at state i at time $t=0$. In order quantify speed and accuracy, we define the splitting probability $\Pi_{R/W}$ as the probability that the first product created is correct (incorrect), assuming that the system starts at state 1 (the free enzyme state E) at time $t=0$:

$$\Pi_{R/W} = \int_0^\infty F_{R/W,1}(t)\,\mathrm{d}t\,. \tag{S13}$$

Naturally, accuracy is quantified by the error rate given by

$$\eta = \frac{\Pi_W}{\Pi_R}, \tag{S14}$$

which is consistent with its traditional definition as the ratio between the product forming rates[22, 23]. The speed (i.e., inverse time) is quantified by the conditional mean first-passage time (MFPT), which is given by the (normalized) first moment of the first-passage probability density

$$\tau = \frac{1}{\Pi_R}\int_0^\infty t F_{R,1}(t)\mathrm{d}t. \tag{S15}$$

Now we present the mathematical formalism used to analytically determine η and τ. According to the definition, the first-passage probability densities of the end states read:

$$\begin{aligned} F_{R,10}(t) = \delta(t), \quad F_{R,11}(t) = 0, \\ F_{W,10}(t) = 0, \quad F_{W,11}(t) = \delta(t), \end{aligned} \tag{S16}$$

where $\delta(t)$ is the Dirac δ function. The time evolution of the first-passage probability densities of the other states $F_{R/W,i}(t)$ $(i=1,2,\ldots,9)$ is governed by the backward master equations, which read:

$$\frac{\mathrm{d}}{\mathrm{d}t}F_{R/W,i}(t) = \sum_{j=1}^{11} k_{i,j}\left[F_{R/W,j}(t) - F_{R/W,i}(t)\right], \quad i=1,2,\ldots,9 \tag{S17}$$

where $k_{i,j}$ denotes the first-order rate of transition from state i to state j and the initial conditions are $F_{R/W,i}(t)=0$ for $i=1,2,\ldots,9$. The transition rates $k_{i,j}$ in the tRNA^{Ile} aminoacylation network are compactly given by:

$$\mathbf{K} = (k_{i,j})_{11\times 11} = \begin{pmatrix} 0 & k_+ & k'_+ & k_{-h1} & k'_{-h1} & k_{-h2} & k'_{-h2} & k_{-h3} & k'_{-h3} & 0 & 0 \\ k_- & 0 & 0 & k_a & 0 & 0 & 0 & 0 & 0 & 0 & 0 \\ k'_- & 0 & 0 & 0 & k'_a & 0 & 0 & 0 & 0 & 0 & 0 \\ k_{h1} & k_{-a} & 0 & 0 & 0 & k_3 & 0 & 0 & 0 & 0 & 0 \\ k'_{h1} & 0 & k'_{-a} & 0 & 0 & 0 & k'_3 & 0 & 0 & 0 & 0 \\ k_{h2} & 0 & 0 & k_{-3} & 0 & 0 & 0 & k_4 & 0 & 0 & 0 \\ k'_{h2} & 0 & 0 & 0 & k'_{-3} & 0 & 0 & 0 & k'_4 & 0 & 0 \\ k_{h3} & 0 & 0 & 0 & 0 & k_{-4} & 0 & 0 & 0 & k_p & 0 \\ k'_{h3} & 0 & 0 & 0 & 0 & 0 & k'_{-4} & 0 & 0 & 0 & k'_p \\ 0 & 0 & 0 & 0 & 0 & 0 & 0 & k_{-p} & 0 & 0 & 0 \\ 0 & 0 & 0 & 0 & 0 & 0 & 0 & 0 & k'_{-p} & 0 & 0 \end{pmatrix}. \tag{S18}$$

While Eqs. S16–S18 in principle can be directly solved for $F_{R/W,i}(t)$, it is usually more convenient to solve the backward master equations by performing a Laplace transformation $\tilde{F}_{R/W,i}(s) = \int_0^\infty F_{R/W,i}(t)e^{-st}\,\mathrm{d}t$. The transformed system obeys the following set of equations:

$$s\tilde{F}_{R/W,i}(s) = \sum_{j=1}^{11} k_{i,j}\left[\tilde{F}_{R/W,j}(s) - \tilde{F}_{R/W,i}(s)\right], \quad i = 1, 2, \ldots, 9 \tag{S19}$$

and

$$\begin{aligned} \tilde{F}_{R,10}(s) &= 1, \quad \tilde{F}_{R,11}(s) = 0 \\ \tilde{F}_{W,10}(s) &= 0, \quad \tilde{F}_{W,11}(s) = 1. \end{aligned} \tag{S20}$$

Equation S19 is a set of linear algebraic equations for $\tilde{F}_{R/W,i}(s)$ that can be solved analytically. The associated splitting probabilities $\Pi_{R/W}$ are given by

$$\Pi_{R/W} = \int_0^\infty F_{R/W,1}(t)\,\mathrm{d}t = \tilde{F}_{R/W,1}(s=0). \tag{S21}$$

The error η is therefore determined as the ratio of the two splitting probabilities

$$\eta = \frac{\Pi_W}{\Pi_R} = \frac{\tilde{F}_{W,1}(0)}{\tilde{F}_{R,1}(0)}. \tag{S22}$$

The conditional MFPT τ is given by the normalized first moment of the first-passage probability density:

$$\tau = \frac{1}{\Pi_R}\int_0^\infty tF_{R,1}(t)\,\mathrm{d}t = -\frac{1}{\Pi_R}\left(\frac{\mathrm{d}\tilde{F}_{R,1}(s)}{\mathrm{d}s}\right)\bigg|_{s=0}. \tag{S23}$$

The symbolic linear algebra calculations based on Eqs. S17–S23 are done in Mathematica. The resulting expressions evaluated for the estimated parameter values are plotted in the main text figures.

B. Forward Master Equations and the Definition of Dissipation

In the forward framework, we use $P_i(t)$ to denote the probability of the enzyme being in chemical state i at time t. The main difference from the backward framework is that states 1, 10, and 11 should be considered to be the same state (i.e. the free enzyme). Therefore, we only have 9 distinct enzyme states. The probabilities of the enzyme being in different states are normalized by the following condition:

$$\sum_{i=1}^{9} P_i(t) = 1, \quad \forall\, t \in \mathbf{R}. \tag{S24}$$

The time-dependent probability flux from state i to state j is given by $J_{i,j}(t) = k_{i,j}P_i(t)$. The time evolution of the probabilities $P_i(t)$ is governed by the forward master equations, which read:

$$\frac{\mathrm{d}P_i(t)}{\mathrm{d}t} = \sum_j \left[k_{j,i}P_j(t) - k_{i,j}P_i(t)\right], \quad i = 1, 2, \ldots, 9. \tag{S25}$$

Note that merging states 1, 10, and 11 reduces the transition rates matrix $\mathbf{K}$ to a 9×9 matrix, which reads:

$$\mathbf{K} = (k_{i,j})_{9\times 9} = \begin{pmatrix} 0 & k_+ & k'_+ & k_{-h1} & k'_{-h1} & k_{-h2} & k'_{-h2} & k_{-h3}+k_{-p} & k'_{-h3}+k'_{-p} \\ k_- & 0 & 0 & k_a & 0 & 0 & 0 & 0 & 0 \\ k'_- & 0 & 0 & 0 & k'_a & 0 & 0 & 0 & 0 \\ k_{h1} & k_{-a} & 0 & 0 & 0 & k_3 & 0 & 0 & 0 \\ k'_{h1} & 0 & k'_{-a} & 0 & 0 & 0 & k'_3 & 0 & 0 \\ k_{h2} & 0 & 0 & k_{-3} & 0 & 0 & 0 & k_4 & 0 \\ k'_{h2} & 0 & 0 & 0 & k'_{-3} & 0 & 0 & 0 & k'_4 \\ k_{h3}+k_p & 0 & 0 & 0 & 0 & k_{-4} & 0 & 0 & 0 \\ k'_{h3}+k'_p & 0 & 0 & 0 & 0 & 0 & k'_{-4} & 0 & 0 \end{pmatrix}. \tag{S26}$$

Setting the right hand side of Equation S25 to zero gives the steady-state probability distributions P_i^{ss}. We can calculate the steady-state probability fluxes $J_{i,j}^{\mathrm{ss}} = k_{i,j}P_i^{\mathrm{ss}}$ (The

superscript ss will be dropped for simplicity). The steady state energy dissipation rate of the system is given by:

$$\sigma_0 = \sum_i (J_i^+ - J_i^-) \ln \frac{J_i^+}{J_i^-}, \tag{S27}$$

where $J_i^\pm$ are the forward/backward steady-state fluxes of the chemical reaction i[19, 24].

It can be shown that the energy dissipation can be decomposed into three parts:

$$\sigma_0 = J_{\text{proof}} \Delta\mu_{\text{ATP}} + J_R \Delta\mu_R + J_W \Delta\mu_W, \tag{S28}$$

where J_{proof} is the sum of all net proofreading fluxes; J_R and J_W are the product formation fluxes for the right and wrong product, respectively. $\Delta\mu_{\text{ATP}} = 29.5\, k_B T$ is the free energy released from ATP hydrolysis into AMP and PP_i under physiological concentrations of ATP, AMP, and PP_i. $\Delta\mu_R = \Delta\mu_p = 9.8\, k_B T$ is the free energy cost of forming a correctly charged isoleucyl-tRNA, namely the difference between the free energy released from the hydrolysis of ATP and that stored in the ester bond connecting tRNA and isoleucine. $\Delta\mu_W$ is the corresponding energy cost for valine, which is typically different from $\Delta\mu_R$. However, since J_W is much smaller than other fluxes, especially J_R, the difference between $\Delta\mu_W$ and $\Delta\mu_R$ has negligible impact on the total dissipation. For the purpose of computing the total dissipation, we can safely ignore the last term in Eq. S28. We study the normalized dissipation rate σ defined as the dissipation rate per correct product formed:

$$\sigma = \frac{\sigma_0}{J_R} = \frac{J_{\text{proof}}}{J_R} \Delta\mu_{\text{ATP}} + \Delta\mu_R + \eta \Delta\mu_W \approx \frac{J_{\text{proof}}}{J_R} \Delta\mu_{\text{ATP}} + \Delta\mu_R. \tag{S29}$$

The symbolic linear algebra calculations based on Eqs. S24–S29 are done in Mathematica. The resulting expressions evaluated for estimated parameter values are plotted in the main text figures.

REFERENCES

[1] M. Ibba and D. Söll, Aminoacyl-tRNA synthesis, Annu. Rev. Biochem. **69**, 617 (2000).

[2] J. Ling, N. Reynolds, and M. Ibba, Aminoacyl-tRNA synthesis and translational quality control, Annu. Rev. Microbiol. **63**, 61 (2009).

[3] N. Cvetesic, M. Bilus, and I. Gruic-Sovulj, The tRNA A76 hydroxyl groups control partitioning of the tRNA-dependent pre- and post-transfer editing pathways in class I tRNA synthetase, J. Biol. Chem. **290**, 13981 (2015).

[4] W. Freist, Isoleucyl-tRNA synthetase: An enzyme with several catalytic cycles displaying variation in specificity and energy consumption, Angew. Chem. Int. Ed. Engl. **27**, 773 (1988).

[5] A. R. Fersht, Editing mechanisms in protein synthesis. Rejection of valine by the isoleucyl-tRNA synthetase, Biochemistry **16**, 1025 (1977).

[6] B. D. Bennett, E. H. Kimball, M. Gao, R. Osterhout, S. J. Van Dien, and J. D. Rabinowitz, Absolute metabolite concentrations and implied enzyme active site occupancy in *Escherichia coli*, Nat. Chem. Biol. **5**, 593 (2009).

[7] F. C. Neidhardt, J. L. Ingraham, and M. Schaechter, *Physiology of the bacterial cell: A molecular approach* (Sinauer Associates, 1990).

[8] H. Dong, L. Nilsson, and C. G. Kurland, Co-variation of tRNA abundance and codon usage in *Escherichia coli* at different growth rates, J. Mol. Biol. **260**, 649 (1996).

[9] K. A. Dittmar, M. A. Sørensen, J. Elf, M. Ehrenberg, and T. Pan, Selective charging of tRNA isoacceptors induced by amino-acid starvation, EMBO Rep. **6**, 151 (2005).

[10] E. Kukko-Kalske, M. Lintunen, M. K. Inen, R. Lahti, and J. Heinonen, Intracellular PPi concentration is not directly dependent on amount of inorganic pyrophosphatase in *Escherichia coli* K-12 cells, J. Bacteriol. **171**, 4498 (1989).

[11] P. A. Frey and A. Arabshahi, Standard free energy change for the hydrolysis of the α,β-phosphoanhydride bridge in ATP, Biochemistry **34**, 11307 (1995).

[12] A. S. Spirin, *Ribosomes* (Springer US, Boston, MA, 1999).

[13] M. Dulic, N. Cvetesic, J. J. Perona, and I. Gruic-Sovulj, Partitioning of tRNA-dependent editing between pre- and post-transfer pathways in class I aminoacyl-tRNA synthetases, J. Biol. Chem. **285**, 23799 (2010).

[14] C. MacDonald, D. Yu, M. Buibas, and G. Silva, Diffusion modeling of ATP signaling suggests a partially regenerative mechanism underlies astrocyte intercellular calcium waves, Front. Neuroeng. **1**, 1 (2008).

[15] T. S. Azarashvili, I. V. Odinokova, O. V. Krestinina, Y. L. Baburina, D. E. Grachev, V. V. Teplova, and E. L. Holmuhamedov, Role of phosphorylation of porine proteins in regulation of mitochondrial outer membrane under normal conditions and alcohol intoxication, Biol. Membr. **28**, 14 (2011).

[16] R. O. Potts, N. C. Ford, and M. J. Fournier, Changes in the solution structure of yeast phenylalanine transfer ribonucleic acid associated with aminoacylation and magnesium binding,

Biochemistry **20**, 1653 (1981).

[17] J. C. Biro, The concept of RNA-assisted protein folding: the role of tRNA, Theor. Biol. Med. Modell. **9**, 10 (2012).

[18] A. Plochowietz, I. Farrell, Z. Smilansky, B. S. Cooperman, and A. N. Kapanidis, In vivo single-RNA tracking shows that most tRNA diffuses freely in live bacteria, Nucleic Acids Res. **45**, 926 (2017).

[19] H. Qian, Open-system nonequilibrium steady state: Statistical thermodynamics, fluctuations, and chemical oscillations, J. Phys. Chem. B **110**, 15063 (2006).

[20] K. Banerjee, A. B. Kolomeisky, and O. A. Igoshin, Elucidating interplay of speed and accuracy in biological error correction, Proc. Natl. Acad. Sci. U. S. A. **114**, 5183 (2017).

[21] J. D. Mallory, A. B. Kolomeisky, and O. A. Igoshin, Trade-offs between error, speed, noise, and energy dissipation in biological processes with proofreading, J. Phys. Chem. B **123**, 4718 (2019).

[22] J. J. Hopfield, Kinetic proofreading: A new mechanism for reducing errors in biosynthetic processes requiring high specificity, Proc. Natl. Acad. Sci. U. S. A. **71**, 4135 (1974).

[23] M. Johansson, M. Lovmar, and M. Ehrenberg, Rate and accuracy of bacterial protein synthesis revisited, Curr. Opin. Microbiol. **11**, 141 (2008).

[24] T. L. Hill, *Free energy transduction in biology* (Academic Press, 1977).